CONF-941115--4

OXIDATION OF SILICON IMPLANTED WITH HIGH-DOSE ALUMINUM

Zunde Yang,* Honghua Du,*+ and Stephen P. Withrow**
*Department of Materials Science and Engineering, Stevens Institute of Technology, Hoboken, NJ 07030
**Oak Ridge National Laboratory, Oak Ridge, TN 37831

ABSTRACT

Si (100) wafers were implanted with Al at 500°C to high doses at multi-energies and were oxidized in 1 atm flowing oxygen at 1000°-1200°C. The morphology, structure, and oxidation behavior of the implanted and oxidized Si were studied using optical microscopy, atomic force microscopy, and cross-sectional transmission electron microscopy in conjunction with selected area electron diffraction and energy dispersive x-ray analysis. Large Al precipitates were formed and embedded near the surface region of the implanted Si. The oxidation rate of the Al-implanted Si wafers was lower than that of virgin Si. The unique morphology of the implanted Si results from rapid Al diffusion and segregation promoted by hot implantation. The reduction of the oxidation rate of Si by Al implantation is attributed to the preferential oxidation of Al and formation of a continuous diffusion barrier of Al_2O_3.

INTRODUCTION

Oxidation studies of Si implanted with various impurities have been documented [1-4]. The list of the impurities includes Pb, Ag, Ti, Co, Fe, Sn, Ge, B, As, and P. In general, the implanted impurities give rise to an increased oxidation rate relative to that observed for unimplanted Si. The mechanism responsible for the accelerated oxidation varies depending upon the phase and structural characteristics of the implanted Si and the segregation behavior of the impurities. For example, impurities such as Pb, Ag, and Ti segregate to the vicinity of the SiO_2/Si interface during oxidation; implantation-induced lattice damage is attributed to the oxidation rate change [1]. Ge is rejected by SiO_2 and is accumulated as a Ge-rich interphase between SiO_2 and Si during oxidation, which modifies the interfacial reaction rate [2]. Impurities such as B segregate into SiO_2 during growth which increases the diffusive process in the oxide [3]. And implants such as As and P readily segregate into Si which accelerate the interfacial reaction [4]. It has been demonstrated that ion implantation provides a unique means to modify the oxidation of silicon and to study the processes responsible for the morphological and structural development during implantation and oxidation treatments.

Documented studies of Al implantation of Si have focused primarily on the structural and electrical characteristics of Si [5,6]. This paper summarizes our investigation of the effect of high-dose Al implantation on the morphology, structure, and oxidation behavior of Si. The processes responsible for the morphological evolution and for the decreased oxidation rate of Al- implanted Si are discussed.

+ To whom correspondence should be addressed

Mat. Res. Soc. Symp. Proc. Vol. 354 © 1995 Materials Research Society

MASTER

DISTRIBUTION OF THIS DOCUMENT IS UNLIMITED

EXPERIMENTAL

Single crystal Si (100) was sequentially implanted with Al using an Extrion high-current implanter to $2.25 \times 10^{17}/cm^2$ at 143 keV, $7.4 \times 10^{16}/cm^2$ at 72 keV, and $3.2 \times 10^{16}/cm^2$ at 35 keV. The substrate temperature was maintained at around 500°C during implantation. The doses and the ion energies were selected to achieve an implant concentration distribution of 20 at.% from the surface to a depth of 350 nm based upon computer simulation using the PROFILE code [7]. The morphological, structural, and phase characteristics of the implanted samples were determined by optical microscopy, atomic force microscopy (AFM), and cross-sectional transmission electron microscopy (XTEM) in conjunction with selected area electron diffraction (SAD) and energy dispersive x-ray (EDX) analysis.

Oxidation of the Al-implanted Si samples was performed in 1 atm dry oxygen flowing at 500 SCCM at 1000°-1200°C. Virgin Si was also oxidized simultaneously for comparison. The oxide thickness was determined by XTEM for implanted samples or by ellipsometry for virgin Si. The samples after oxidation were also investigated using XTEM, SAD, and EDX.

RESULTS AND DISCUSSION

Shown in Figs. 1(a) and 1(b) are optical and AFM micrographs of the Al-implanted Si sample. Fig. 1(a) indicates the presence of precipitates with a large population density and varying size distribution (0.5-2 μm) in the surface region of the implanted Si. The precipitates are embedded in the Si sample with the free surface slightly below that of the substrate, as depicted in Fig. 1(b).

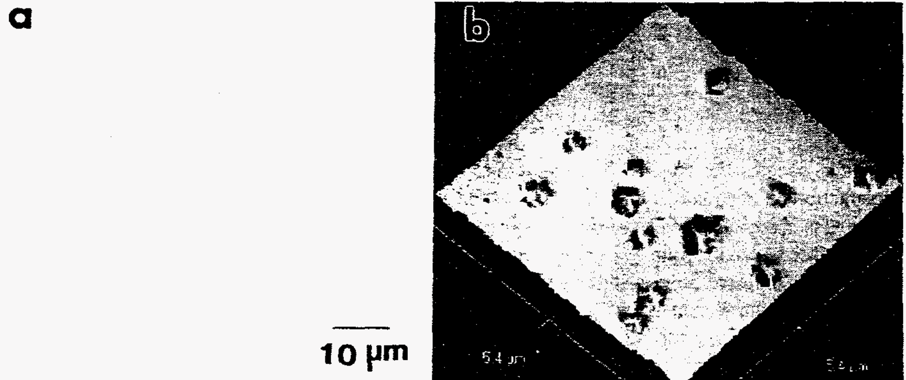

Figure 1. (a) Optical and (b) atomic force micrograph of Al-implanted Si.

A bright-field XTEM image from the Al-implanted Si is presented in Fig. 2(a). SAD patterns taken from regions A and B in Fig. 2(a) are shown in Figs. 2(b) and 2(c), respectively. The band of dark contrast in Fig. 2(a), which extends from the surface to about 650 nm beneath, corresponds to the implanted region. The thickness of the implanted region nearly doubles that of the value from simulation by the PROFILE code. It is postulated that this inconsistency may arise from the channeling effect as well as from Al diffusion during implantation. The dark contrast results from implantation-

DISCLAIMER

This report was prepared as an account of work sponsored by an agency of the United States Government. Neither the United States Government nor any agency thereof, nor any of their employees, makes any warranty, express or implied, or assumes any legal liability or responsibility for the accuracy, completeness, or usefulness of any information, apparatus, product, or process disclosed, or represents that its use would not infringe privately owned rights. Reference herein to any specific commercial product, process, or service by trade name, trademark, manufacturer, or otherwise does not necessarily constitute or imply its endorsement, recommendation, or favoring by the United States Government or any agency thereof. The views and opinions of authors expressed herein do not necessarily state or reflect those of the United States Government or any agency thereof.

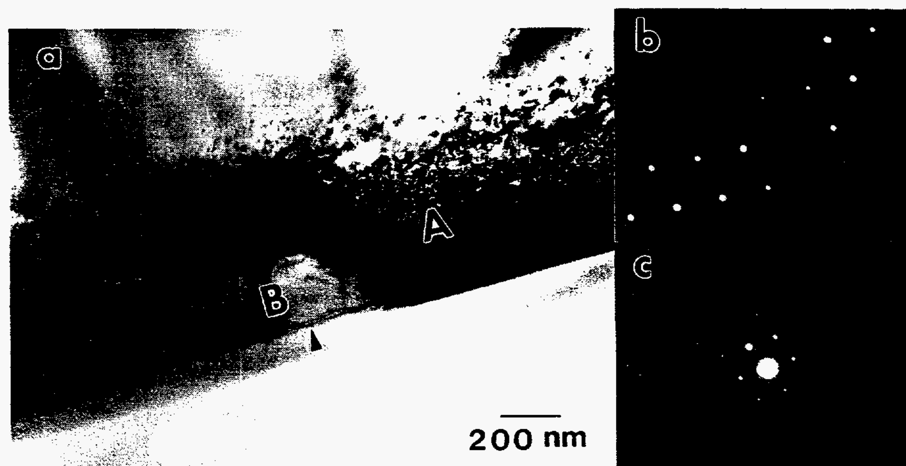

Figure 2. (a) Bright-field XTEM image and SAD patterns from (b) region A and (c) region B shown in (a) of Al-implanted Si.

induced lattice damage of the Si sample. Due to sufficient dynamic lattice recovery during ho implantation the Si retained not only its crystallinity, but also its (100) orientation in the implantec region, as indicated in Fig. 2(b). No additional deflection spots are present in Fig. 2(b), which suggest that region A in Fig. 2(a) is single crystal Si.

Fig. 2(a) reveals the cross-sectional morphology of the precipitate (region B) illustrated in th optical and AFM micrographs. EDX analysis (spectrum not shown here) indicated the presence c only Al in the pocket. The SAD pattern from this region (Fig. 2(c)) corresponds to single crystal A with a [011] zone axis (same as the Si substrate). Early studies of Al implantation of Si wer conducted at temperatures below 50°C; Al precipitates are observed only upon annealing the implantec Si above 600°C [5,6]. Al has a very low solubility and is a fast diffusing species in single crystal S [6,8]. Ion-beam irradiation is known to significantly enhance the rate of diffusion and segregation c implants even in binary covalent systems such as SiC [9,10]. The combined thermal and irradiatio effects are therefore responsible for the formation of Al precipitates in Si implanted with high-doses o Al at the temperature used here. The morphology of the Al precipitates concurs with an equilibriun configuration which minimizes surface/interface energy of the system.

Al-implanted Si exhibits an oxidation behavior quite different from virgin Si in terms of th oxidation rate as well as the characteristics of the oxidation products. Summarized in Table 1 are th thickness values of the oxidation layers grown on Al-implanted (determined by XTEM) and on virgi Si (measured by ellipsometry) under various oxidation conditions. The oxidized samples are relativel smooth despite the distinct surface morphology of the as-implanted Si. One exception is the sampl oxidized at 1200°C which has a thicker oxide around the Al pocket region. For this reason, a thicknes range is given in this table for the sample oxidized at this temperature. As seen in Table 1, th oxidation rate of Si is reduced by Al implantation, in contrast to implantation by many other metalli species [1-4].

Table 1. Thickness of the oxidation layer grown on Al-implanted and virgin Si under various oxidation conditions.

Oxidation Temperature (°C)	Oxidation Time (hours)	Oxide Thickness (nm)	
		Implanted Si	Pure Si
1000	6.0	110	185
1100	6.0	220	345
1200	5.0	270-400	400

The oxidation results of Al-implanted and virgin Si indicate that Al plays a unique role in modifying the oxidation process of Si. The effect of Al implantation on the morphological and phase development of the oxidation layer has been investigated using XTEM and EDX. Shown in Fig. 3 is a bright-field XTEM image of the Al-implanted Si sample after oxidation at 1000°C. The region with dark contrast (indicated by arrows) corresponds to the oxidation layer (110 nm thick) and the contrast difference clearly suggests the low ion-milling rate of the oxide phase. While SAD analysis of this region was unsuccessful due to a thickness limit, EDX analysis of this region, shown in Fig. 4, indicated the presence of only Al and O. These results strongly suggest that the oxide formed is Al_2O_3. Although the oxidation layer grown at 1000°C is relatively smooth, XTEM analysis of certain regions where large Al pockets were once present indicated some structural and phase heterogeneity with Al_2O_3 grains extending into Si beneath the average baseline of the oxide/substrate interface.

Figure 3. Bright-field XTEM image of Al-implanted Si after oxidation at 1000°C.

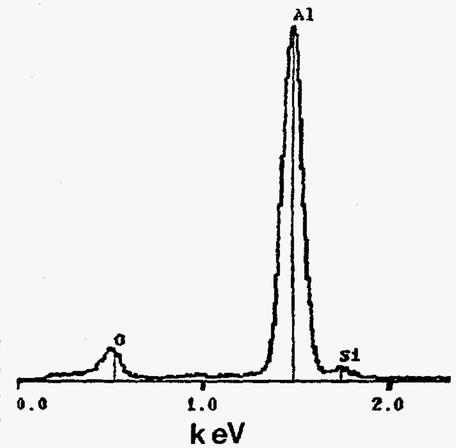

Figure 4. EDX spectrum from the oxidation layer grown on Al-implanted Si at 1000°C.

The oxidation treatment at 1000°C resulted in the formation of precipitates with sizes ranging from nano to submicron dimensions in the Si substrate beneath the oxidation layer, as shown in Fig. 3. EDX analysis of the relatively large precipitates revealed the presence of only Al. In addition, the oxidation treatment also led to the removal of implantation-induced lattice damage in the implanted and

unoxidized region as evidenced by the light contrast in this region (Fig. 3). This observation o formation of precipitates and damage recovery upon high-temperature treatment is consistent wit previous work [5,6].

Shown in Figs. 5 and 6 are bright-field XTEM images of Al-implanted Si samples oxidized a 1100°C and 1200°C, respectively. As illustrated, the oxidation layer consists of two sub-layers in bot cases. Based upon the EDX analysis of these regions, the outer layer of dark contrast is Al_2O_3 and th inner layer of light contrast is SiO_2. The region beneath the oxidation layer after the oxidatio treatment at these two temperatures exhibits structural features similar to those after 1000°C oxidatio exposure.

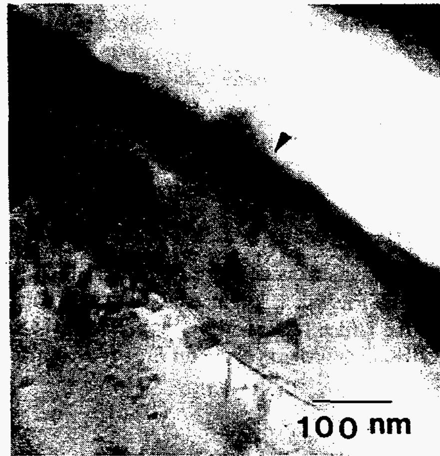

Figure 5. Bright-field XTEM image of Al-implanted Si after oxidation at 1100°C.

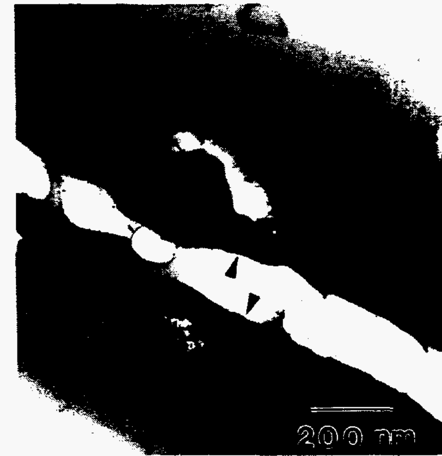

Figure 6. Bright-field XTEM image of Al-implanted Si after oxidation at 1200°C.

This investigation strongly indicates that oxidation of Al-implanted Si proceeds first b oxidation of Al to form a continuous layer of Al_2O_3 with the reaction interface as a diffusion sink for A and the Al pockets in the surface region as an Al reservoir. Once Al in the pockets is depleted for th formation of Al_2O_3, oxidation of Si will take place to form SiO_2. These two stages of oxidation of A implanted Si can be understood from the thermodynamic and kinetic standpoints. Thermodynamical speaking, the Gibbs free energy of the formation of Al_2O_3 is about 25% more negative compared wit SiO_2 per mole of oxygen in the temperature range of 1000°-1200°C. Al should be selectively (c preferentially) oxidized by oxygen when co-existing with Si. The much stronger affinity of Al fc oxygen than Si has been illustrated through its effective role in gettering oxygen in single crystal Si an the reduction of SiO_2 by Al [5,6]. Kinetically speaking, Al is in a molten state at the oxidatic temperatures. The surface as well as bulk diffusivity of Al will be high, which are the favorab conditions for the formation of a continuous Al_2O_3 layer and rapid refurbishment of Al from the A pockets. The depletion of Al will lead to formation of vacancy and ultimately microscopic porosity i the Al/Si interface region where Al pockets once existed. This vacancy or porosity generation proce is postulated to be responsible for the very light contrast observed in the oxidation layer in the regic where a pocket of Al has been consumed by oxidation. Al-implanted Si exhibits a reduced rate c

oxidation compared to virgin Si. Specifically, the thickness ratio of the oxidation layers formed on Al-implanted and on virgin Si is 0.60 at 1000°C (6 hours), 0.64 at 1100°C (6 hours), and 0.68-1.0 at 1200°C (5 hours). The reduction in the oxidation rate can be attributed to the formation of a diffusion barrier of Al_2O_3 through which oxygen diffuses less rapidly than through SiO_2 [11].

CONCLUSIONS

Ion implantation of Si with high-dose Al at 500°C resulted in the formation of a unique structure and morphology. Si retained its single crystallinity and orientation; numerous pockets of single crystal Al were also formed, both of which can be attributed to irradiation-enhanced diffusion and segregation. Oxidation of Al-implanted Si resulted in the formation of a continuous layer of Al_2O_3, and when Al in the Al pocket is consumed, the formation of SiO_2. These oxidation processes are consistent with thermodynamic and kinetic considerations. The preferential oxidation of Al and formation of an Al_2O_3 diffusion barrier are responsible for the reduced oxidation rate of Al-implanted Si compared with virgin Si.

ACKNOWLEDGMENT

This work was sponsored by the National Science Foundation under Grant No. MSS-9110256 and managed by Dr. Jorn Larsen-Basse, director of the NSF Surface Engineering and Tribology Program. Work done at Oak Ridge was supported by the Office of Basic Energy Sciences, U.S. Department of Energy, under contract DE-AC05-84OR21400 with Martin Marietta Energy Systems, Inc.

REFERENCES

1. O.W. Holland, C.W. White, and S.J. Pennycook, J. Mater. Res., vol. 3, 898 (1988).
2. O.W. Holland, C.W. White, and D. Fathy, Apply. Phys. Lett., 51, 520 (1987).
3. B.E. Deal and M. Sklar, J. Electrochem. Soc., 112, 430 (1965).
4. J.F. Gotzlich, K. Haberger, H. Ryssel, H. Kranz, and E. Traumuler, Radiation Effects, 47, 203 (1980).
5. D.K. Sadana, M.H. Norcott, R.G. Wilson, and U. Dahmen, Appl. Phys. Lett., 49, 1169 (1986).
6. P. Bruesch, H. Halder, P. Kluge, J. Rhyner, P. Roggwiller, Th. Stockmeier, F. Stucki, and H.J. Wiesmann, J. Appl. Phys., 68, 2226 (1990).
7. Commercial software by Implant Sciences, Corp., Danvers, MA.
8. B.J. Baliga, Modern Power Devices (Wiley, New York, 1987) p.29.
9. I.L. Singer and J.H. Wandass, *Structure-Property Relationships in Surface-Modified Ceramics*, edited by C.J. McHargue (Kluwer Academic Publishers, 1989) p.199.
10. Z. Yang, H. Du, M. Libera, and I.L. Singer, in this proceedings.
11. W.D. Kingery, H.K. Bowen, and D.R. Uhlmann, *Introduction to Ceramics*, 2nd Edition (John Wiley & Sons, Inc., New York, 1976).